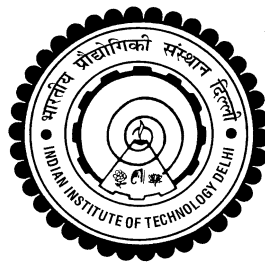


**ANALYSIS OF GRAVITY DAM-FOUNDATION SYSTEM  
FOR JOINTED ROCK FOUNDATIONS WITHOUT AND  
WITH SHEAR SEAMS**

**KANUPREIYA**



**DEPARTMENT OF CIVIL ENGINEERING  
INDIAN INSTITUTE OF TECHNOLOGY DELHI  
NEW DELHI-110016, INDIA**

**JANUARY 2019**

© Indian Institute of Technology Delhi (IITD), New Delhi, 2019

**ANALYSIS OF GRAVITY DAM-FOUNDATION SYSTEM  
FOR JOINTED ROCK FOUNDATIONS WITHOUT AND  
WITH SHEAR SEAMS**

*by*

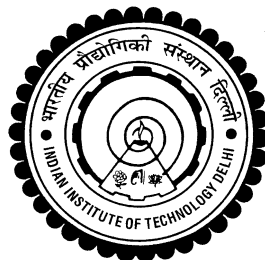
KANUPREIYA

**Department of Civil Engineering**

Submitted

**in fulfillment of the requirements of the degree of Doctor of Philosophy**

to the



**INDIAN INSTITUTE OF TECHNOLOGY DELHI**

**JANUARY 2019**

*Dedicated to*  
*my husband: Amit Gupta and*  
*my son: Shivansh Gupta*

## CERTIFICATE

This is to certify that the thesis entitled “Analysis of Gravity Dam–Foundation System for Jointed Rock Foundations Without and With Seams” submitted by **Ms. Kanupreiya** to the Indian Institute of Technology Delhi, is a record of the bonafide research work carried out by her under our supervision and guidance. This thesis work, in our opinion, has reached the standard, fulfilling the requirements for **Doctor of Philosophy** degree. The research report and the results presented in this thesis have not been submitted, in part or full, to any other university or institute, for the award of any degree or diploma.

(Dr. K. G. Sharma)

Emeritus Professor

(Dr. Bappaditya Manna)

Associate Professor

Department of Civil Engineering

Indian Institute of Technology Delhi New Delhi – 110016

INDIA

## ACKNOWLEDGEMENTS

I would like to express my sincere gratitude to **Dr. K. G. Sharma** and **Dr. Bappaditya Manna**, Professors, Department of Civil Engineering, Indian Institute of Technology Delhi for their constant effort throughout the work by continuous encouragement, meticulous guidance and inspiration during this research work. I am grateful for their co-operation and kind help rendered from time to time.

My sincere thanks are to **Shri R.K. Gupta**, Chairman and Managing Director, WAPCOS Ltd. and **Shri Anupam Mishra**, Executive Director, WAPCOS Ltd. for giving me this opportunity to pursue the research work in addition to the office duties. My heart filled thanks to **Dr. R. K. Gupta**, Chief Engineer, Central Water Commission for his guidance, insights and suggestions. I would also like to express my gratitude to **Ms. P. Sumana**, Chief Engineer, WAPCOS Ltd. for her immense support throughout the research work.

A special thanks for my in-laws **Shri Ashok Gupta** and **Smt. Geeta Gupta** who have always loved me and have unconditionally supported me in every sphere of life. I would like to extend my gratitude to my parents, **Shri Yogendra Pal** and **Smt. Manju Pal** for their blessings and the trust they have shown in me. I would like to thank my pillar of support, my husband, **Mr. Amit Gupta**, without whose love and support, this research work was not possible. I would like to express my deepest love for my son, **Master Shivansh** who stood by me with his unconditional love and allowed me to spend time doing research, in the time that rightfully belonged to him. A loving thanks to my sister, **Ms. Tanya Singhal** who although is younger than me, but supports me like an elder sister, is a friend and much more. I can never thank God enough for the love and support extended by my family.

I would also like to thank **Dr. Aditya Singh** and **Ms. Rajani Sharma** for constructive discussions and suggestions for the best performing of the research and their valuable opinions during the writing process.

I would also like to thank all those who have rendered help directly or indirectly during the entire research. Last but not least, I would like to thank all my friends and relatives for their continuous encouragement for the research.

*Kanupreiya*  
(Kanupreiya)

## ABSTRACT

At present, India's installed capacity in the hydropower sector is approximately 44.47 GW out of total power capacity of 326.84 GW (CEA, 2018). Therefore, a substantial development of the hydropower is required which significantly depends on construction of dams. Concrete gravity dams (referred as dams) transmit large loads to the foundation, which requires detailed analysis of dam-foundation system. Rock mass comprises of joints and shear seams and hence distinct element models, DEM, that incorporates deformable blocks are required (Cundal, 1992).

The detailed project reports of 40 hydroelectric projects in the Himalayan region are reviewed and the apparent dips of the set of joints of these projects evaluated to access the combination of joint orientations used for analysis in this study.

The dam and foundation are modelled as two discrete blocks, which are interacting through an interface between them. Analysis is carried out for two loading conditions, viz., (i) Loading condition 'A' (construction condition), *LCA*, i.e., construction of dam completed but no water in reservoir and no tail water, and (ii) Modified loading condition 'B', *LCB*, i.e., full reservoir level, with extreme uplift, assuming the drainage holes to be inoperative. For *LCB* both coupled hydro-mechanical analysis, *LCB<sub>c</sub>*, and uncoupled hydro-mechanical analysis, *LCB<sub>u</sub>*, (or mechanical analysis) are carried out.

To study the effect of joints and shear seams, dam-foundation analysis is carried out idealizing the foundation rock as (a) a discontinuum jointed rock mass foundation with one or two sets of joints, (b) a continuum rock foundation with shear seam, and (c) a discontinuum rock foundation with shear seam. For the present study elasto-plastic analyses has been carried out for 29,612 cases using the software Universal Distinct Element Code, UDEC (Itasca, 2011).

Analysis of the dam-foundation system with single set of joints are carried out to study the effect of (a) single set of joints: by varying the joint spacing,  $s$ , joint orientation,  $\theta_j$  of the foundation joints; (b) foundation joint stiffness: by varying joint normal stiffnesses,  $k_n$ , and joint shear stiffnesses,  $k_s$  and (c) dam-foundation interface joint stiffness by varying the dam-foundation interface normal stiffness,  $k_{ni}$ , and dam-foundation interface shear stiffness,  $k_{si}$ .

As expected, it is observed that the major principal stresses are maximum at the heel for *LCA* and at the toe for *LCB* (both *LCB<sub>c</sub>* and *LCB<sub>u</sub>*). For *LCB<sub>c</sub>*, the uplift pressure distribution is non-linear and varies with the variation of joint orientation. For most cases for *LCB<sub>c</sub>*, the factor of safety is higher than that from the conventional analysis. It is also observed that for both *LCA* and *LCB<sub>c</sub>*, major principal stress and crest displacement increase as joint spacing reduces, for all  $\theta_j$ . For

values of  $\theta_j$  from  $0^\circ$  to  $30^\circ$  and  $105^\circ$  to  $180^\circ$ ,  $LCA$  is the critical condition for stresses while for values of  $\theta_j$  from  $30^\circ$  to  $105^\circ$ ,  $LCB_c$  is critical. For  $LCA$ , the displacements are minimum for sub-horizontal joints and maximum for sub-vertical joints. For  $LCB_c$ , the  $x$ -displacements of the crest are minimum for sub-horizontal joint sets and maximum for sub-vertical joint sets while the  $y$ -displacements of the crest are maximum for sub-horizontal joint sets and minimum for sub-vertical joint sets. It is observed that stresses and displacements under both loading conditions are dependent on the product of  $k_n$  and  $s$ , and, for any value of  $k_n \cdot s$  greater than Young's modulus of intact rock,  $E_r$ , i. e.,  $k_n \cdot s > E_r$ , the stresses and displacements do not change with further increase in  $k_n \cdot s$ . It is generally observed that as the ratio  $k_n/k_s$  increases, the stress and displacement increases.

The behaviour of rock foundation with two sets of joints is evaluated by varying the joint spacing,  $s$ , joint set orientation,  $\theta_j$ , and included joint angle,  $\theta_i$ . The joint set spacing for both joint sets are assumed equal. Critical joint set combinations for major principal stress are observed as  $0^\circ$ - $120^\circ$  and  $120^\circ$ - $150^\circ$  for  $LCA$ , and  $0^\circ$ - $90^\circ$  and  $0^\circ$ - $150^\circ$  for  $LCB_c$ . Crest displacements are observed to be critical for  $60^\circ$ - $90^\circ$  and  $30^\circ$ - $60^\circ$  for  $LCA$ . For  $LCB_c$ , critical joint combinations for  $x$ -displacements are  $0^\circ$ - $120^\circ$ ,  $30^\circ$ - $90^\circ$  and for  $y$ -displacements are  $60^\circ$ - $90^\circ$ ,  $30^\circ$ - $60^\circ$ .

To study the effect of seam in the dam-foundation system, analysis has been carried out by idealising the foundation as equivalent continuum by varying the seam width, seam orientation,  $\theta_s$ , with respect to the upstream horizontal and seam strength properties namely, seam cohesion,  $c_s$ , and angle of friction,  $\phi_s$ . The locations of the seam are considered at Heel ( $HI$ ), Heel-Center ( $HC$ ), Center ( $C$ ), Center-Toe ( $CT$ ) and Toe ( $T$ ).

It is observed that due to the presence of a seam, the stresses and displacements are affected in the vicinity of the seam, in the dam and foundation. The deformation at the mid-point of the seam,  $\delta_{y_s}$ , at the dam base is compared with the deformation at the same location without the seam,  $\delta_y$ . A seam influence factor ( $I_f$ ) defined as the ratio of  $\delta_{y_s}$  to  $\delta_y$  is calculated for each case, to study the impact of the seam.

Seam orientation of  $90^\circ$  and  $120^\circ$  is observed to be most critical for  $LCA$  and  $LCB_c$  respectively. A seam at the heel ( $HI$ ) of the dam is most critical for both loading conditions. In all cases, the seam influence factor increases with increase in the seam width. For both loading conditions it is observed that as value of  $c_s$  or  $\phi_s$  decreases, values of  $\delta_{y_s}$  and  $I_f$  increase. The effect of change in  $c_s$  or  $\phi_s$  is greater for smaller values of  $c_s$  or  $\phi_s$ .

In order to study the effect of shear seam on a jointed rock foundation, and, to calculate the optimum depth of plug for dental treatment, analyses are carried out for a gravity dam on a jointed rock foundation with a single set of joints along with shear seam and plugs for dams of different heights. Twelve different joint set orientations ( $\theta_j$ ), and a spacing of 2 m are considered for foundation joints. Seam of four different widths are considered at different locations below dam base. Analysis is carried out for both  $LCA$  and  $LCB_c$ .

Additional analysis are carried out with concrete plugs of 4 different depths for each seam considered and plug efficiency curves are developed. The optimum plug depth is defined as the plug depth where the rate of change of plug efficiency reduces to 1%. A study of the optimum plugs for all cases considered showed that the impact of  $\theta_s, \theta_j$  and seam location is negligible on the value of optimum plug depth for seam of various widths.

In order to develop an empirical equation for the optimum plug depth required for dental treatment of shear seam, the optimum plug depth is calculated for different dam heights and seam widths.

Based on the assessment of the impact of various parameters on the optimum plug depth, the relevant variables affecting plug depth, namely, dam height and seam width, have been identified, and an empirical relationship is proposed through regression analysis. The plug depth calculated from the derived empirical relationship has also been compared against other similar equations available for plug depth.

Numerical validation of empirical equation for optimum plug depth is carried out for variation in joint spacing; variation of ratio of Young's modulus of intact rock blocks to that of dam concrete,  $E_r/E_c$ ; and varying the ratio of Young's modulus of rock blocks to that of shear seam blocks,  $E_r/E_s$ . Impact of variation in each of the parameters on the optimum plug depth is studied.

It is concluded from the above study that the empirical relationship developed in the present study is suitable for calculating the optimum depth of plug which should be provided for any given seam width and dam height.

## सार

वर्तमान में, भारत की 326.84 GW की कुल बिजली क्षमता में से हाइड्रोपावर क्षेत्र की इंस्टॉलड क्षमता लगभग 44.47 GW है (CEA, 2018)। इसलिए, हाइड्रोपावर के पर्याप्त विकास की आवश्यकता है, जो डैम के निर्माण पर काफी निर्भर करता है। कंक्रीट ग्रेविटी डैम (डैम के नाम में संदर्भित) विशाल लोड्स को फॉउण्डेशन में ट्रांसमिट करते हैं, जिसके लिए डैम-फॉउण्डेशन सिस्टम के विस्तृत विश्लेषण की आवश्यकता होती है। रॉक मास में जॉइंट्स और शीअर सीम शामिल होती हैं, और इसलिए डिस्टिंक्ट एलिमेंट मॉडल (डीईएम, DEM), जिसमें डिफोरमेबल ब्लॉक शामिल हैं, की आवश्यकता होती है (Cundal, 1992)।

इस अध्ययन में हिमालयी क्षेत्र की 40 हाइड्रोपावर परियोजनाओं की डिटेल्ड प्रोजेक्ट रिपोर्ट्स की समीक्षा की गई है, और इन परियोजनाओं के जॉइंट सेट्स के अपैरेंट डिप्स का मूल्यांकन किया गया है, और उनका उपयोग इस अध्ययन में विश्लेषण हेतु उपयोग किए जाने वाले जॉइंट ओरिएन्टेशन तक पहुंचने के लिए किया गया है।

डैम और फॉउण्डेशन को दो डिस्क्रीट ब्लॉकों के रूप में मॉडल किया गया है, जो उनके बीच एक इंटरफेस के माध्यम से परस्पर इंटरैक्शन कर रहे हैं। विश्लेषण दो लोडिंग कंडीशंस के लिए किया गया है, नामतः (i) लोडिंग कंडीशन 'A' (कंस्ट्रक्शन कंडीशन),  $LCA$ , अर्थात्, पूर्णतया निर्मित डैम, जिसके रिज़ेर्वायर में पानी नहीं है और टेल वाटर भी नहीं है, और (ii) मॉडिफाइड लोडिंग कंडीशन 'B',  $LCB$ , अर्थात्, पूर्ण रिज़ेर्वायर स्तर, एक्सट्रीम अपलिफ्ट वाली स्थिति, ड्रेनेज होल्स निष्क्रिय मान लिए गए हैं।  $LCB$  के लिए कपल्ड हाइड्रो-मैकेनिकल एनालिसिस,  $LCB_c$ , और अन्-कपल्ड हाइड्रो-मैकेनिकल एनालिसिस,  $LCB_u$ , (या मैकेनिकल एनालिसिस), ये दोनों किए गए हैं।

जॉइंट्स और शीअर सीमों के प्रभाव का अध्ययन करने हेतु, डैम-फॉउण्डेशन सिस्टम का विश्लेषण फॉउण्डेशन के रॉक को तीन स्थितियों में आइडियलाइज़ कर के किया गया है, क्रमशः (क) जॉइंट्स के एक या दो सेटों के साथ एक डिस्कॉन्टीन्यूअम जॉइंटेड रॉक मास फाउंडेशन, (ख) शीअर सीम के साथ एक कॉन्टीन्यूअम रॉक फाउंडेशन, और (ग) शीअर सीम के साथ एक डिस्कॉन्टीन्यूअम रॉक फाउंडेशन। वर्तमान अध्ययन के लिए यूनिवर्सल डिस्टिंक्ट एलिमेंट कोड, यूडीईसी (UDEEC) सॉफ्टवेयर (Itasca, 2011) के उपयोग द्वारा 29,612 परिस्थितियों का इलास्टो-प्लास्टिक एनालिसिस किया गया है।

जॉइंट्स के सिंगल सेट के साथ डैम-फॉउण्डेशन सिस्टम का विश्लेषण किया गया है, निम्नलिखित स्थितियों के प्रभावों का अध्ययन करने हेतु: (क) जॉइंट्स का सिंगल सेट: फॉउण्डेशन के जॉइंट्स के विभिन्न जॉइंट स्पेसिंग्स,  $s$ , तथा विभिन्न जॉइंट ओरिएन्टेशन,  $\theta_j$ , के प्रभाव का अध्ययन; (ख) फॉउण्डेशन के जॉइंट्स की जॉइंट स्टिफनेस: विभिन्न जॉइंट नॉर्मल स्टिफनेस,  $k_n$ , तथा विभिन्न जॉइंट शीअर स्टिफनेस,  $k_s$ , के प्रभाव का अध्ययन, और (ग) डैम-फॉउण्डेशन के इंटरफेस की इंटरफेस जॉइंट स्टिफनेस: विभिन्न इंटरफेस नॉर्मल स्टिफनेस,  $k_{ni}$ , तथा विभिन्न इंटरफेस शीअर स्टिफनेस,  $k_{si}$ , के प्रभाव का अध्ययन किया गया है।

जैसा कि अपेक्षित था, यह देखा गया है कि मेजर प्रिंसिपल स्ट्रेस  $LCA$  के लिए डैम के हील पर और  $LCB$  (दोनों  $LCB_c$  और  $LCB_u$ ) के लिए डैम के टो पर अधिकतम होते हैं।  $LCB_c$  के लिए, अपलिफ्ट प्रेशर डिस्ट्रीब्यूशन नॉन-लीनियर है और जॉइंट ओरिएन्टेशन की भिन्नता के साथ बदलता रहता है। अधिकांश परिस्थितियों में कन्वेंशनल एनालिसिस की तुलना में  $LCB_c$  का

फैक्टर ऑफ़ सेफ्टी अधिक पाया गया है। यह भी देखा गया है कि  $LCA$  और  $LCB_c$  दोनों स्थितियों में, सभी  $\theta_j$  के लिए, जॉइंट स्पेसिंग कम होने से मेजर प्रिंसिपल स्ट्रेस और क्रेस्ट डिस्प्लेसमेंट दोनों में वृद्धि होती है।  $\theta_j$  के मान  $0^\circ$  से  $30^\circ$  और  $105^\circ$  से  $180^\circ$  के लिए, स्ट्रेस के लिए क्रिटिकल कंडीशन  $LCA$  पायी गयी है, जबकि  $\theta_j$  के मान  $30^\circ$  से  $105^\circ$  के लिए, स्ट्रेस के लिए क्रिटिकल कंडीशन  $LCB_c$  पायी गयी है।  $LCA$  के लिए, न्यूनतम डिस्प्लेसमेंट स्थिति सब-हॉरिज़ॉन्टल जॉइंट्स के लिए, और अधिकतम डिस्प्लेसमेंट स्थिति सब-वर्टिकल जॉइंट्स के लिए पायी गयी है।  $LCB_c$  के लिए, डैम के क्रेस्ट का x-डिस्प्लेसमेंट सब-हॉरिज़ॉन्टल जॉइंट्स के सेट के लिए न्यूनतम और सब-वर्टिकल जॉइंट्स के सेट के लिए अधिकतम पाया गया है, जबकि डैम के क्रेस्ट का y-डिस्प्लेसमेंट सब-हॉरिज़ॉन्टल जॉइंट्स के सेट के लिए अधिकतम और सब-वर्टिकल जॉइंट्स के सेट के लिए न्यूनतम पाया गया है। यह देखा गया है कि दोनों लोडिंग कंडीशंस में स्ट्रेस और डिस्प्लेसमेंट  $k_n$  और  $s$  के गुणनफल ( $k_n \cdot s$ ) पर निर्भर होते हैं, और, इन्टैक्ट रॉक के यंग मॉड्युलस,  $E_r$ , से अधिक  $k_n \cdot s$  के किसी भी मूल्य के लिए, अर्थात्,  $k_n \cdot s > E_r$  की स्थिति में, स्ट्रेस और डिस्प्लेसमेंट  $k_n \cdot s$  के मूल्य में वृद्धि के साथ नहीं बदलता। यह आमतौर पर देखा गया है कि जैसे-जैसे  $k_n/k_s$  का अनुपात बढ़ता है, स्ट्रेस और डिस्प्लेसमेंट भी बढ़ता है।

जॉइंट्स के दो सेट से युक्त रॉक फाउंडेशन के व्यवहार का मूल्यांकन जॉइंट स्पेसिंग,  $s$ , जॉइंट सेट ओरिएन्टेशन,  $\theta_j$ , और इनक्लूडेड जॉइंट एंगल,  $\theta_i$ , के विभिन्न मूल्यों को लेकर किया गया है। जॉइंट्स के दोनों सेटों के लिए जॉइंट स्पेसिंग को समान माना गया है। मेजर प्रिंसिपल स्ट्रेस के लिए क्रिटिकल जॉइंट सेट कॉम्बिनेशन,  $LCA$  के लिए  $0^\circ$ - $120^\circ$  और  $120^\circ$ - $150^\circ$ , तथा  $LCB_c$  के लिए  $0^\circ$ - $90^\circ$  और  $0^\circ$ - $150^\circ$  देखे गए हैं। क्रेस्ट डिस्प्लेसमेंट  $LCA$  के लिए  $60^\circ$ - $90^\circ$  और  $30^\circ$ - $60^\circ$  पर क्रिटिकल देखे गए हैं।  $LCB_c$  के लिए क्रिटिकल जॉइंट कॉम्बिनेशन x-डिस्प्लेसमेंट के लिए  $0^\circ$ - $120^\circ$ ,  $30^\circ$ - $90^\circ$  तथा y-डिस्प्लेसमेंट के लिए  $60^\circ$ - $90^\circ$ ,  $30^\circ$ - $60^\circ$  हैं।

डैम-फाउण्डेशन सिस्टम में सीम के प्रभाव का अध्ययन करने हेतु, फाउण्डेशन को एक्विवैलेन्ट कॉन्टीन्यूअम के आदर्शरूप कर, सीम विड्थ, अपस्ट्रीम हॉरिज़ॉन्टल के साथ सीम ओरिएन्टेशन,  $\theta_s$ , तथा सीम स्ट्रेंथ प्रॉपर्टीज़ नामतः सीम कोहेशन,  $c_s$ , और एंगल ऑफ़ फ्रिक्शन,  $\phi_s$ , के विभिन्न मूल्यों को लेकर विश्लेषण किया गया है। सीम की लोकेशंस डैम के हील (HI), हील-सेंटर (HC), सेंटर (C), सेंटर-टो (CT) और टो (T) पर मानी गयीं हैं।

यह देखा गया है कि एक सीम की उपस्थिति के कारण, डैम और फाउण्डेशन में, सीम के आसपास के क्षेत्र का स्ट्रेस और डिस्प्लेसमेंट प्रभावित होते हैं। डैम बेस पर सीम के मध्य-बिंदु पर होने वाली डीफ़ॉर्मेशन,  $\delta_{ys}$ , की तुलना उसी स्थान पर बिना सीम की स्थिति में होने वाली डीफ़ॉर्मेशन,  $\delta_y$ , के साथ की गई है। सीम इम्प्लुएंस फैक्टर,  $I_f$ , को  $\delta_{ys}$  से  $\delta_y$  के अनुपात के रूप में परिभाषित किया गया है, और इसकी गणना प्रत्येक परिस्थिति के लिए की गई है, ताकि सीम के प्रभाव का अध्ययन किया जा सके।

$LCA$  एवं  $LCB_c$  के लिए क्रमशः  $90^\circ$  एवं  $120^\circ$  ओरिएन्टेशन की सीम क्रिटिकल देखी गयी है। दोनों लोडिंग कंडीशंस के लिए सीम की क्रिटिकल लोकेशन डैम के हील (HI) पर देखी गई है। सभी परिस्थितियों में सीम इम्प्लुएंस फैक्टर सीम विड्थ में वृद्धि के साथ बढ़ता जाता है। दोनों लोडिंग कंडीशंस के लिए देखा गया है कि जैसे-जैसे  $c_s$  और  $\phi_s$  का मूल्य कम होता है, वैसे-वैसे  $\delta_{ys}$  और  $I_f$  के मूल्य में वृद्धि होती है।  $c_s$  और  $\phi_s$  में परिवर्तन का प्रभाव  $c_s$  और  $\phi_s$  के छोटे मूल्यों के लिए अधिक होता है।

जॉइंटेड रॉक फाउंडेशन पर शीअर सीम के प्रभाव का अध्ययन करने हेतु, एवं, डेंटल ट्रीटमेंट के लिए ऑप्टिमम प्लग डेपथ की गणना करने हेतु, शीअर सीम और प्लग सहित जॉइंट्स के सिंगल सेट से युक्त जॉइंटेड रॉक फाउंडेशन वाले ग्रेविटी डैम की विभिन्न डैम हाइट्स के लिए विश्लेषण किए गए हैं। फाउंडेशन के जॉइंट सेट ओरिएन्टेशन के बारह अलग-अलग मूल्य एवं जॉइंट स्पेसिंग का मूल्य 2 मीटर माना गया है। डैम बेस के नीचे सीम विभिन्न लोकेशंस पर एवं चार विभिन्न विड्थ्स की मानी गयी है। विश्लेषण  $LCA$  एवं  $LCB_c$  दोनों के लिए किया गया है।

प्रत्येक सीम के लिए कंक्रीट प्लग की 4 विभिन्न डेपथ्स के लिए अतिरिक्त विश्लेषण किया गया है, और प्लग एफिशिएंसी कर्व्स विकसित किए गए हैं। ऑप्टिमम प्लग डेपथ को प्लग की उस डेपथ के रूप में परिभाषित किया गया है जिस डेपथ पर प्लग एफिशिएंसी के परिवर्तन की दर 1% तक कम हो जाती है। विश्लेषण की सभी परिस्थितियों के लिए पाई गई ऑप्टिमम प्लग डेपथ के मूल्यों के अध्ययन से यह दर्शाया गया कि विभिन्न विड्थ्स के सीमों के लिए ऑप्टिमम प्लग डेपथ के मूल्यों पर  $\theta_s, \theta_j$  और सीम लोकेशन का प्रभाव नगण्य है।

शीअर सीम के डेंटल ट्रीटमेंट के लिए आवश्यक ऑप्टिमम प्लग डेपथ के मूल्य की एक इम्पीरिकल इक्वेशन विकसित करने हेतु, अलग-अलग डैम हाइट्स और सीम विड्थ्स के लिए ऑप्टिमम प्लग डेपथ की परिगणना की गई है।

ऑप्टिमम प्लग डेपथ पर विभिन्न पैरामीटर्स के प्रभाव के मूल्यांकन के आधार पर प्लग डेपथ को प्रभावित करने वाले उचित वेरिएबल्स, नामतः, डैम हाइट और सीम विड्थ, की पहचान की गई है, और रिग्रेशन एनालिसिस के माध्यम से एक इम्पीरिकल रिलेशनशिप प्रस्तावित की गई है। डिस्ट्रिब्यूटड इम्पीरिकल रिलेशनशिप से गणना की गई प्लग डेपथ की तुलना प्लग डेपथ के लिए उपलब्ध अन्य समान एक्वेशन्स से भी की गई है।

ऑप्टिमम प्लग डेपथ के लिए विकसित इम्पीरिकल इक्वेशन की न्यूमेरिकल वेलिडेशन निम्न परिस्थितियों में की गई है : विभिन्न जॉइंट स्पेसिंग्स के लिए; इन्टैक्ट रॉक ब्लॉक एवं डैम कंक्रीट के यंग मॉड्युलस के अनुपात ( $E_r/E_c$ ) के विभिन्न मूल्यों के लिए; तथा, रॉक ब्लॉक एवं शीअर सीम ब्लॉक के यंग मॉड्युलस के अनुपात ( $E_r/E_s$ ) के विभिन्न मूल्यों के लिए। ऑप्टिमम प्लग डेपथ पर विभिन्न पैरामीटर्स में भिन्नता के प्रभाव का अध्ययन किया गया है।

उपरोक्त अध्ययन से यह निष्कर्ष निकाला गया है कि वर्तमान अध्ययन में विकसित इम्पीरिकल रिलेशनशिप किसी भी डैम हाइट और सीम विड्थ के लिए प्रदान किए जाने वाले प्लग की ऑप्टिमम डेपथ की गणना हेतु उपयुक्त है।

## TABLE OF CONTENTS

<b>CERTIFICATE</b>	<b>i</b>
<b>ACKNOWLEDGEMENT</b>	<b>iii</b>
<b>ABSTRACT</b>	<b>v</b>
<b>TABLE OF CONTENTS</b>	<b>ix</b>
<b>LIST OF FIGURES</b>	<b>xvii</b>
<b>LIST OF TABLES</b>	<b>xxvii</b>
<b>LIST OF SYMBOLS AND ACRONYMS</b>	<b>xxxii</b>
<b>CHAPTER 1 INTRODUCTION</b>	<b>1</b>
1.1 GENERAL	1
1.2 OBJECTIVES AND SCOPE OF WORK	5
1.3 ORGANISATION OF THE THESIS	6
<b>CHAPTER 2 LITERATURE REVIEW</b>	<b>7</b>
2.1 INTRODUCTION	7
2.2 CONVENTIONAL DESIGN METHOD	8
2.3 STABILITY CRITERIA	10
2.3.1 Resistance against sliding	10
2.3.2 Resistance against overturning	13
2.4 EQUIVALENT MATERIAL PROPERTIES	14
2.5 STRENGTH PARAMETERS	15
2.5.1 Shear Strength of Intact Rock	16
2.5.1.1 <i>Mohr-Coulomb Failure Criterion</i>	<i>16</i>
2.5.1.2 <i>Hoek-Brown Criterion</i>	<i>16</i>
2.5.2 Shear Strength of Joints	17

2.6	EFFECT OF JOINTS IN FOUNDATION	18
2.7	THE JOINT CHARACTERISTICS	20
2.8	SEEPAGE, UPLIFT AND PORE PRESSURES	22
2.9	IMPORTANCE OF FOUNDATION TREATMENT	24
2.10	SHEAR SEAMS IN DAM-FOUNDATIONS	25
2.10.1	Treatment of dam-foundation with shear seams	26
2.10.1.1	<i>Treatment of large seams</i>	26
2.10.1.2	<i>Treatment of sub-horizontal weak seams</i>	30
2.11	OTHER STABILIZATION TECHNIQUES	31
2.12	FOUNDATION PROBLEMS OF SOME LARGE DAMS:	32
2.13	DAM-FOUNDATION INTERACTION	32
2.14	LIMITATIONS OF PREVIOUS STUDIES	32
2.15	SCOPE OF WORK	43
<b>CHAPTER 3</b>	<b>DESIGN METHODOLOGY AND DISTINCT ELEMENT MODELLING</b>	<b>45</b>
3.1	INTRODUCTION	45
3.2	NUMERICAL MODELING	46
3.2.1	Modelling of dam and foundation system	46
3.2.1.1	<i>Physical models</i>	46
3.2.1.2	<i>Mathematical models</i>	47
3.3	UNIVERSAL DISTINCT ELEMENT CODE	51
3.4	FORMULATION OF DISTINCT ELEMENT METHOD	53
3.4.1	Equations of motion	53
3.4.2	Momentum balance in DEM	54
3.4.3	Energy balance in DEM	55
3.5	CONSTITUTIVE MODELS	55
3.5.1	Block constitutive models	55

3.5.1.1	<i>Yield and potential functions</i>	57
3.5.2	Constitutive models for joints	57
3.5.2.1	<i>Coulomb slip model</i>	58
3.5.2.2	<i>Rock joint representation</i>	61
3.5.3	Boundary Conditions	63
3.5.4	Fluid flow in joints	63
3.6	PROPERTIES REQUIRED FOR ANALYSIS USING UDEC	65
3.7	VERIFICATION EXAMPLES -COMPARISON OF RESULTS OF UDEC AND RS <sup>2</sup>	66
3.7.1	Problem definition:	66
3.7.2	Comparison of results	70
3.7.2.1	<i>Principal stresses</i>	70
3.7.2.2	<i>Displacement</i>	73
3.8	CLOSURE	75
<b>CHAPTER 4</b>	<b>MODELING THE DAM-FOUNDATION SYSTEM</b>	<b>77</b>
4.1	GENERAL	77
4.2	GEOLOGICAL EVALUATION OF GRAVITY DAM- FOUNDATIONS IN HIMALAYAN REGION	77
4.3	BASIC PROBLEM GEOMETRY	81
4.4	LOADING CONDITIONS	82
4.5	ESTIMATION OF MATERIAL PROPERTIES	84
4.6	ANALYSIS OF DAM-FOUNDATION SYSTEM	85
4.6.1	Case I	86
4.6.2	Case II	89
4.6.3	Case III	92
4.6.4	Case IV	93
4.7	SIGN CONVENTION FOR PRESENT STUDY	100
4.8	CLOSURE	100

<b>CHAPTER 5</b>	<b>ELASTO-PLASTIC ANALYSIS OF DAM ON FOUNDATION WITH SINGLE SET OF JOINTS</b>	<b>101</b>
5.1	GENERAL	101
5.2	BASIC PROBLEM GEOMETRY	101
5.3	ANALYSIS	101
5.3.1	Material Properties	102
5.3.2	Cases Studied	102
5.4	RESULTS AND DISCUSSIONS	104
5.4.1	Case (I a) - Effect of joint set orientation and joint set spacing	104
5.4.1.1	<i>Effect on uplift at the dam–foundation interface</i>	104
5.4.1.2	<i>Effect on factor of safety against sliding</i>	107
5.4.1.3	<i>Stress response of dam–foundation system</i>	109
5.4.1.4	<i>Deformation response of dam–foundation system</i>	124
5.4.2	Case (I b) – Effect of foundation joint stiffness	140
5.4.2.1	<i>Stress response of dam–foundation system</i>	140
5.4.2.2	<i>Deformation response of dam–foundation system</i>	145
5.4.3	Case (I c) – Effect of dam–foundation interface joint stiffness	154
5.4.3.1	<i>Stress response of dam–foundation system</i>	154
5.4.3.2	<i>Deformation response of dam–foundation system</i>	157
5.5	SUMMARY	161
<b>CHAPTER 6</b>	<b>ELASTO-PLASTIC ANALYSIS OF DAM ON FOUNDATION WITH TWO SETS OF JOINTS</b>	<b>165</b>
6.1	GENERAL	165
6.2	BASIC PROBLEM GEOMETRY	165
6.3	ANALYSIS	165

6.4	RESULTS AND DISCUSSIONS	167
6.4.1	Effect on uplift pressure at the base of the dam	167
6.4.2	Effect on Factor of Safety against Sliding	170
6.4.3	Stress-deformation response of dam-foundation system for a typical case for joint set combination 30°-120° and joint set spacing 2 m.	172
6.4.4	Stress deformation response for a constant included angle between joint sets, with varying orientation of the first joint set	177
6.4.5	Stress-deformation response for a given orientation of one joint set, with varying included angle between the two joint sets	190
6.4.6	Comparison of stress-deformation response for $LCB_c$ and $LCB_u$	197
6.5	SUMMARY	203
<b>CHAPTER 7</b>	<b>SHEAR SEAMS IN EQUIVALENT CONTINUUM ROCK FOUNDATION</b>	<b>205</b>
7.1	GENERAL	205
7.2	BASIC PROBLEM GEOMETRY	205
7.3	ANALYSIS	205
7.3.1	Loading conditions	207
7.3.2	Material properties	207
7.3.3	Details of study	207
	7.3.3.1 <i>Effect of seam width, seam location and orientation</i>	207
	7.3.3.2 <i>Effect of material properties of seam.</i>	208
7.3.4	Method of analysis	209
7.4	RESULTS	210
7.4.1	Effect of location, orientation and width of the seam	210
	7.4.1.1 <i>Effect of seam width and orientation</i>	210
	7.4.1.2 <i>Effect of seam location and orientation</i>	213

7.4.2	Effect of cohesion ( $c_s$ ) and angle of internal friction of the seam ( $\phi_s$ )	233
7.4.2.1	<i>Effect of seam cohesion (<math>c_s</math>), for a given angle of internal friction of the seam (<math>\phi_s</math>)</i>	233
7.4.2.2	<i>Effect of angle of internal friction of the seam (<math>\phi_s</math>) for a given seam cohesion (<math>c_s</math>)</i>	242
7.4.3	Seam influence factors ( $I_f$ ) for different combinations of seam width, seam orientation ( $\theta_s$ ) and seam location across different values of $c_s$ and $\phi_s$	253
7.5	SUMMARY	257
<b>CHAPTER 8</b>	<b>SHEAR SEAMS IN JOINTED ROCK FOUNDATION</b>	<b>261</b>
8.1	GENERAL	261
8.2	BASIC PROBLEM GEOMETRY	262
8.3	ANALYSIS	262
8.3.1	Details of study	264
8.3.2	Method of analysis	268
8.3.2.1	<i>Effect of seam in jointed rock foundation with single set of joints</i>	268
8.3.2.2	<i>Estimation of optimum plug depth for seam in jointed rock foundation with single set of joints</i>	268
8.4	RESULTS	269
8.4.1	Effect of shear seam location, seam width, seam orientation and joint set orientation	269
8.4.1.1	<i>Effect of seam width</i>	279
8.4.1.2	<i>Effect of seam orientation</i>	289
8.4.1.3	<i>Effect of seam location</i>	292
8.4.1.4	<i>Effect of joint set orientation</i>	294
8.4.2	Methodology for estimating optimum plug depth	298
8.4.3	Determination of optimum plug depth for a 100 m high dam	301
8.4.3.1	<i>Optimum plug depth for a typical case</i>	
8.4.3.2	<i>Optimum plug depth for critical seam condition</i>	303
8.4.4	Impact of various parameters on optimum plug depth	305

8.4.4.1	<i>Impact of seam width</i>	305
8.4.4.2	<i>Impact of loading condition</i>	305
8.4.4.3	<i>Impact of seam orientation</i>	306
8.4.4.4	<i>Impact of seam location</i>	306
8.4.4.5	<i>Impact of joint set orientations, <math>\theta_s</math></i>	307
8.4.5	Optimum plug depth for different dam heights	307
8.4.6	Empirical relation between optimum plug depth, dam height and seam width	314
8.4.7	Comparison of various equations for plug depth	319
8.4.8	Validation of empirical equation, Eq. (8.7)	321
8.4.8.1	<i>Comparison of observed optimum plug depth and calculated plug depth for validation cases</i>	322
8.4.8.2	<i>Impact of variation in joint set spacing, <math>E_r/E_c</math> and <math>E_r/E_s</math> on the optimum plug depths</i>	322
8.5	CONCLUSIONS	325
<b>CHAPTER 9</b>	<b>CONCLUSIONS</b>	<b>329</b>
9.1	GENERAL	329
9.2	CONCLUSIONS	329
9.2.1	Dam on jointed rock foundation	329
9.2.1.1	<i>Effect on uplift at the dam–foundation interface</i>	330
9.2.1.2	<i>Effect on factor of safety against sliding</i>	331
9.2.1.3	<i>Stress-deformation response for jointed rock foundation with single set of joints</i>	332
9.2.1.4	<i>Stress-deformation response for jointed rock foundation with two sets of joints</i>	335
9.2.2	Dam on rock foundation with shear seam	335
9.2.2.1	<i>Stress-deformation response for shear seam on rock foundation idealized as equivalent continuum</i>	337
9.2.2.2	<i>Shear seam in rock foundation with single set of joints</i>	338
9.2.2.3	<i>Optimum plug depth</i>	339
9.3	SIGNIFICANT CONTRIBUTION OF PRESENT RESEARCH	340
9.4	SCOPE FOR FURTHER STUDIES	341

<b>REFERENCES</b>	<b>343</b>
<b>BRIEF BIODATA</b>	<b>359</b>

## LIST OF FIGURES

Fig. 1.1	Power scenario in India	2
Fig. 1.2	Region wise Hydropower potential scenario in India	3
Fig. 2.1	Typical cross section of a gravity dam	9
Fig. 2.2	Geological conditions leading to sliding failure in dam-foundations (Wahlstrom, 1974)	13
Fig. 2.3	Narrowing and deepening of the stress bulb in single set of jointed rock mass (Goodman, 1989)	18
Fig. 2.4	Line loads inclined arbitrarily on a half space in transversely isotropic rock mass. (Bray, 1977)	19
Fig. 2.5	Pressure bulbs for arbitrary inclined joints in transversely isotropic half space. (Bray, 1977)	20
Fig. 2.6	Diagram showing tensile stress at the base of the structure over the low modulus zone and stress concentration in the adjoining rock (Sharma and Varma, 1998).	28
Fig. 2.7	Diagram showing transfer of applied load to foundation rock by provision of concrete plug (Sharma and Varma, 1998).	28
Fig. 3.1	Example of a UDEC model (Itasca, 2011)	52
Fig. 3.2	Contacts and domains between two deformable blocks (Itasca 2011)	58
Fig. 3.3	Basic joint behaviour model used in UDEC (Itasca, 2011)	60
Fig. 3.4	Contacts between two rigid blocks (Itasca 2011)	61
Fig. 3.5	Definition of rounded corners in UDEC (Itasca 2011)	62
Fig. 3.6	Fluid-solid interactions in discontinua (Itasca, 2011)	64
Fig. 3.7	Relation between hydraulic aperture and joint normal stress (Itasca, 2011)	65
Fig. 3.8	Gravity Dam on Intact Rock foundation.	67
Fig. 3.9	100 m high gravity dam on intact rock foundation.-Problem geometry	68
Fig. 3.10	100 m high Gravity Dam on Intact Rock foundation.- RS <sup>2</sup> Model under LCB	69
Fig. 3.11	100 m Gravity Dam on Intact Rock foundation-Zoning of Dam, UDEC Model along with boundary conditions (zones magnified 3 times)	69
Fig. 3.12	Major and Minor Principal stresses in dam for <i>LCA</i> - Intact Rock foundation using UDEC and RS <sup>2</sup>	71
Fig. 3.13	Major and Minor Principal stress in dam for <i>LCB</i> -Intact Rock foundation using UDEC and RS <sup>2</sup>	72
Fig. 3.14	<i>x</i> -displacement and <i>y</i> -displacement contours in dam for <i>LCA</i> -Intact Rock foundation using UDEC and RS <sup>2</sup>	73

Fig. 3.15	$x$ -displacement and $y$ -displacement contours in dam for LCB-Intact Rock foundation using UDEC and RS <sup>2</sup>	74
Fig. 4.1	Distribution of joint set orientation in foundation of gravity dams	80
Fig. 4.2	Distribution of joint set orientation in foundation of gravity dams	80
Fig. 4.3	Basic problem geometry-100 m high dam on rock foundation	82
Fig. 4.4	Schematic diagram for the cases of analysis	86
Fig. 4.5	Schematic diagram for Case I - 100 m high dam on jointed rock foundation with single set of joints	87
Fig. 4.6	Schematic diagram for Case (I a) - 100 m high dam on jointed rock foundation with single set of joints -study of effect of joint orientation and spacing	88
Fig. 4.7	Schematic diagram for Case (I b) - 100 m high dam on jointed rock foundation with single set of joints -study of effect of foundation joint stiffness ratio	90
Fig. 4.8	Schematic diagram for Case (I c) - 100 m high dam on jointed rock foundation with single set of joints at 2 m spacing - study of effect of dam-foundation interface joint stiffness	91
Fig. 4.9	Schematic diagram for 100 m high dam on rock foundation with two sets of joints	92
Fig. 4.10	Seam Locations - 100 m high dam on continuum rock foundation showing different seam locations considered for analysis	93
Fig. 4.11	Schematic diagram for 100 m high dam on equivalent continuum rock foundation without and with shear seam	94
Fig. 4.12	Schematic diagram for dam on foundation with single set of joints with shear seam and without and with plug	95
Fig. 4.13	Schematic diagram for 100 m high dam on foundation with single set of joints with shear seam and without and with plug	97
Fig. 4.14	Schematic diagram for dam of different heights on foundation with single set of joints without and with shear seam and without and with plug	98
Fig. 4.15	Schematic diagram for validation cases – Variation of joint set spacing and Material moduli for various dam heights	99
Fig. 5.1	Basic problem geometry-100 m dam on rock foundation with single set of joints	102
Fig. 5.2	Joint set orientations ( $\theta_j$ ) considered for single set of joints in foundation	103
Fig. 5.3	Variation of uplift pressure along the dam-foundation interface for different $\theta_j$ and $s = 2$ m	105
Fig. 5.4	Variation of uplift pressure along the dam-foundation interface for different $\theta_j$ and $s = 0.5$ m	105
Fig. 5.5	Percentage decrease in uplift for various $\theta_j$ and $s$ , for LCB <sub>c</sub> over LCB <sub>u</sub>	108

Fig. 5.6	Percentage increase in factor of for various $\theta_j$ and $s$ for $LCB_c$ over $LCB_u$	110
Fig. 5.7	Major and minor principal stresses at the heel and toe of the dam for $LCA$	110
Fig. 5.8	Major and minor stress contours for $\theta_j = 0^\circ$ , $s = 2$ m for $LCA$	111
Fig. 5.9	Major and minor stress contours for $\theta_j = 0^\circ$ , $s = 0.5$ m for $LCA$	111
Fig. 5.10	Major and minor stress contours for $LCA$ , $\theta_j = 90^\circ$ , $s = 0.5$ m and 2 m	113
Fig. 5.11	Major and minor stress contours for $LCA$ , $\theta_j = 0^\circ$ , $s = 0.5$ m and 2 m	113
Fig. 5.12	Major and minor principal stresses at the heel and toe of the dam for $LCB_c$	115
Fig. 5.13	Major and minor stress contours for $LCB_c$ , for , $\theta_j = 45^\circ$ , $s = 0.5$ m and 2 m	116
Fig. 5.14	Major and minor stress contours for $LCB_c$ , for , $\theta_j = 0^\circ$ , $s = 2$ m	117
Fig. 5.15	Variation of principal stresses at the heel and toe for various $\theta_j$ and $s$ , for loading condition 'A' and 'B'	117
Fig. 5.16	Major and minor stress contours for $LCB_u$ for $\theta_j = 45^\circ$ , $s = 0.5$ m	119
Fig. 5.17	Major and minor stress contours for $LCB_c$ and $LCB_u$ , horizontal joint at different joint set spacing	120
Fig. 5.18	Major and minor stress contours for $LCB_c$ and $LCB_u$ , 0.5 m joint set spacing and different $\theta_j$	121
Fig. 5.19	Variation of $\sigma_1^T$ and $\sigma_1^H$ with variation in $\theta_j$ and $s$ for $LCB_c$ and $LCB_u$	122
Fig. 5.20	$x$ - and $y$ -displacements of the dam for $LCA$ for horizontal joints in foundation with 2 m and 0.5 m joint set spacing	125
Fig. 5.21	$x$ - and $y$ -displacements of the dam for $LCA$ for vertical joints in foundation with 2 m and 0.5 m joint set spacing	126
Fig. 5.22	Variation of $x$ - and $y$ -displacements at dam crest for various $\theta_j$ and $s$ , for $LCA$	127
Fig. 5.23	Variation of $x$ -displacements of the dam-heel and toe for various $\theta_j$ and $s$ for $LCA$	128
Fig. 5.24	Variation of $y$ -displacements of the dam heel and toe for various $\theta_j$ and $s$ , for $LCA$	129
Fig. 5.25	$x$ - and $y$ -displacements of the dam for $LCB_c$ for 0.5 m and 2 m joint set spacing, horizontal joints in foundation	130
Fig. 5.26	$x$ - and $y$ -displacement contours $LCB_c$ , vertical joint at 0.5 and 2 m spacing	131
Fig. 5.27	$x$ - and $y$ -displacements at the crest of the dam for $LCB_c$ for various $\theta_j$ and $s$	132
Fig. 5.28	Incremental $x$ - and $y$ -displacements at the crest of the dam for $LCB_c$ over and above the effect of $LCA$	132

Fig. 5.29	$x$ -displacements of the dam at the heel and toe for $LCB_c$ for various joint set spacing and joint set orientations	134
Fig. 5.30	$y$ -displacements of the dam at the heel and toe for $LCB_c$ for various joint set spacing and joint set orientations	134
Fig. 5.31	$x$ - and $y$ -displacements of the dam for $LCB_u$ for 0.5 m and 2 m joint set spacing, horizontal joints in foundation	136
Fig. 5.32	$x$ - and $y$ -displacements of the dam for $LCB_u$ for 2 m joint set spacing, vertical joints in foundation	137
Fig. 5.33	$x$ -displacements at the crest of the dam for $LCB_u$ and $LCB_c$ , for various $\theta_j$ and $s$	138
Fig. 5.35	$x$ -displacements of the dam at the heel and toe for $LCB_u$ for various $\theta_j$ and $s$	139
Fig. 5.36	$y$ -displacements of the dam at the heel and toe for $LCB_u$ for various $\theta_j$ and $s$	140
Fig. 5.37	Major principal stress at the heel of the dam for $LCA$ , for different combinations of joint stiffness ratios with joint set orientations, and 1 m joint set spacing	141
Fig. 5.38	Major principal stress at the heel of the dam for $LCA$ , for different combinations of joint stiffness ratios with joint set orientations, and 2 m joint set spacing	141
Fig. 5.39	$\sigma_1^T$ for $LCB_c$ , for different combinations of $k_n/k_s$ with joint set orientations, and 1 m joint set spacing	143
Fig. 5.40	$\sigma_1^T$ for $LCB_c$ , for different combinations of joint stiffness ratios with joint set orientations, and 2 m joint set spacing	143
Fig. 5.41	$x$ -displacement at the crest of the dam for $LCA$ , for different combinations of joint stiffness ratios with joint set orientations, and 1 m joint set spacing	146
Fig. 5.42	$x$ -displacement at the crest of the dam for $LCA$ , for different combinations of joint stiffness ratios with joint set orientations, and 2 m joint set spacing	147
Fig. 5.43	$y$ -displacement at the crest of the dam for $LCA$ , for different combinations of joint stiffness ratios with $\theta_j$ , and 1 m joint set spacing	147
Fig. 5.44	$y$ -displacement at the crest of the dam for $LCA$ , for different combinations of joint stiffness ratios with $\theta_j$ , and 2 m joint set spacing	148
Fig. 5.45	Deformed shape of the dam-foundation system (magnified 100 times) for $LCA$ , for $\theta_j = 45^\circ$ and $135^\circ$ and $s = 1$ m, for $k_n = 2000$ MPa/m and $k_n/k_s = 10$	148
Fig. 5.46	$x$ -displacement at the crest of the dam for $LCB_c$ , for different combinations of joint stiffness ratios with joint set orientations, and 1 m joint set spacing	151

Fig. 5.47	$x$ -displacement at the crest of the dam for $LCB_c$ , for different combinations of joint stiffness ratios with joint set orientations, and 2 m joint set spacing	151
Fig. 5.48	$y$ -displacement at the crest of the dam for $LCB_c$ , for different combinations of joint stiffness ratios with joint set orientations, and 1 m joint set spacing	152
Fig. 5.49	$y$ -displacement at the crest of the dam for $LCB_c$ , for different combinations of joint stiffness ratios with joint set orientations, and 2 m joint set spacing	152
Fig. 5.50	Major Principal stress at the heel of the dam for different $k_{ni}$ and $k_{ni}/k_{si}$ at various $\theta_j$ and $s = 2$ m for $LCA$	155
Fig. 5.51	Major Principal stress (MPa) at the toe of the dam for different $k_{ni}$ and $k_{ni}/k_{si}$ at various joint set orientations for $LCB_c$	156
Fig. 5.52	$x$ -displacement at the crest of the dam for $LCA$ , for different combinations of $k_{ni}/k_{si}$ with joint set orientations	157
Fig. 5.53	$y$ -displacement at the crest of the dam for $LCA$ , for different combinations of $k_{ni}/k_{si}$ with joint set orientations	158
Fig. 5.54	$x$ -displacement at the crest of the dam for $LCB_c$ , for different combinations of interface stiffness ratios with joint set orientations	160
Fig. 5.55	$y$ -displacement at the crest of the dam for $LCB_c$ , for different combinations of interface stiffness ratios with joint set orientations	160
Fig. 6.1	Basic problem geometry - 100 m dam on granitic rock foundation with two sets of joints for typical case of joint at $30^\circ$ and $120^\circ$ and joint set spacing of 2 m	166
Fig. 6.2	Variation of uplift pressure along the dam-foundation interface for different joint set spacings and joint set combination of $30^\circ$ - $120^\circ$	169
Fig. 6.3	Variation of uplift pressure along the dam-foundation interface for different joint set combinations and a constant joint set spacing of 0.5 m	169
Fig. 6.4	Percentage increase in factor of safety for various joint set spacings and joint set combinations for $LCB_c$ and $LCB_u$	172
Fig. 6.5	Major and minor principal stress in dam for $LCA$ -for joint set orientations $30^\circ$ - $120^\circ$ and 2 m joint set spacing	173
Fig. 6.6	Major and Minor Principal stress in dam foundation for $LCA$ -jointed rock foundation with two sets of joints with joint set orientations $30^\circ$ - $120^\circ$	174
Fig. 6.7	Major and Minor Principal stress in dam $LCB_c$ for joint set orientations $30^\circ$ - $120^\circ$ and joint set spacing 2 m.	174
Fig. 6.8	Major and Minor Principal stress in dam foundation for $LCB_c$ and $LCB_u$ - for joint set orientations $30^\circ$ - $120^\circ$ and joint set spacing 2 m	175
Fig. 6.9	$x$ -and $y$ -displacement contours for $LCA$ for joint set combination $30^\circ$ - $120^\circ$ and joint set spacing 2 m	176

Fig. 6.10	$x$ -and $y$ -displacement contours in dam for $LCB_c$ for joint set combination $30^\circ$ - $120^\circ$ , $\theta_i=90^\circ$ and joint set spacing 2 m	176
Fig.6.11	Major principal stress at heel and toe, and $x$ -and $y$ -displacements at crest, heel and toe, for various combinations of $\theta_j$ and $s$ , for $LCA$ and $LCB_c$ , for $\theta_i=30^\circ$	178
Fig.6.12	Major principal stress at heel and toe, and $x$ -and $y$ -displacements at crest, heel and toe, for various combinations of $\theta_j$ and $s$ , for $LCA$ and $LCB_c$ , for $\theta_i=60^\circ$	179
Fig. 6.13	Major principal stress at heel and toe, and $x$ -and $y$ -displacements at crest, heel and toe, for various combinations of $\theta_j$ and $s$ , for $LCA$ and $LCB_c$ , for $\theta_i=90^\circ$	180
Fig.6.14	Major principal stress at heel and toe, and $x$ -and $y$ -displacements at crest, heel and toe, for various combinations of $\theta_j$ and $s$ , for $LCA$ and $LCB_c$ , for $\theta_i=120^\circ$	181
Fig.6.15	Major principal stress at heel and toe, and $x$ -and $y$ -displacements at crest, heel and toe, for various combinations of $\theta_j$ and $s$ , for $LCA$ and $LCB_c$ , for $\theta_i=150^\circ$	182
Fig.6.15	Major principal stress at heel and toe, and $x$ -and $y$ -displacements at crest, heel and toe, for various combinations of $\theta_j$ and $s$ , for $LCA$ and $LCB_c$ , for $0^\circ$ orientation of the one joint set	191
Fig.6.17	Major principal stress at heel and toe, and $x$ -and $y$ -displacements at crest, heel and toe, for various combinations of $\theta_j$ and $s$ , for $LCA$ and $LCB_c$ , for $30^\circ$ orientation of the one joint set	192
Fig.6.18	Major principal stress at heel and toe, and $x$ -and $y$ -displacements at crest, heel and toe, for various combinations of $\theta_j$ and $s$ , for $LCA$ and $LCB_c$ , for $60^\circ$ orientation of the one joint set	193
Fig.6.19	Major principal stress at heel and toe, and $x$ -and $y$ -displacements at crest, heel and toe, for various combinations of $\theta_j$ and $s$ , for $LCA$ and $LCB_c$ , for $90^\circ$ orientation of the one joint set	194
Fig.6.20	Major principal stress at heel and toe, and $x$ -and $y$ -displacements at crest, heel and toe, for various combinations of $\theta_j$ and $s$ , for $LCA$ and $LCB_c$ , for $120^\circ$ orientation of the one joint set	195
Fig.6.21	Major principal stress at heel and toe, and $x$ -and $y$ -displacements at crest, heel and toe, for various combinations of $\theta_j$ and $s$ , for $LCA$ and $LCB_c$ , for $150^\circ$ orientation of the one joint set	196
Fig.6.22	Major principal stress at toe and $x$ -and $y$ -displacements at crest, for various combinations of $\theta_j$ and $s$ , for $LCB_c$ and $LCB_u$ , for $30^\circ/150^\circ$ and $60^\circ$ included angle	199
Fig.6.23	Major principal stress at toe and $x$ -and $y$ -displacements at crest, for various combinations of $\theta_j$ and $s$ , for $LCB_c$ and $LCB_u$ , for $90^\circ$ and $120^\circ$ included angle	200

Fig. 7.1	Terminology used for seams	206
Fig. 7.2	Problem Geometry – 100 m dam on continuum rock foundation showing seam located at the heel of dam of different seam orientations	206
Fig. 7.3	Seam Locations - 100 m dam on equivalent continuum rock foundation showing different seam locations considered for analysis	207
Fig. 7.4	Impact of $\theta_s$ on $\delta_{ys}$ and $I_f$ , for $LCA$ and $LCB_c$ for seams of different widths at the heel of dam	214
Fig. 7.5	Impact of $\theta_s$ on $\delta_{ys}$ and $I_f$ , for $LCA$ and $LCB_c$ for seams of different widths at the heel-centre of dam	215
Fig. 7.6	Impact of $\theta_s$ on $\delta_{ys}$ and $I_f$ , for $LCA$ and $LCB_c$ for seams of different widths at the center of dam	215
Fig. 7.7	Impact of $\theta_s$ on $\delta_{ys}$ and $I_f$ , for $LCA$ and $LCB_c$ for seams of different widths at the center-toe of dam	216
Fig. 7.8	Impact of $\theta_s$ on $\delta_{ys}$ and $I_f$ , for $LCA$ and $LCB_c$ for seams of different widths at the toe of dam	216
Fig. 7.9	Major principal stress and stress trajectories for 10 m wide seam at different orientations at the heel of the dam, for $LCA$	218
Fig. 7.10	$y$ -displacements for 10 m wide seam at different orientations at the heel of the dam, for $LCA$	219
Fig. 7.11	Major principal stress and stress trajectories for 10 m wide seam at different orientations at the heel of the dam, for $LCB_c$	220
Fig. 7.12	$y$ -displacements for 10 m wide seam at different orientations at the heel of the dam, for $LCB_c$	221
Fig. 7.13	Impact of seam location on $I_f$ , for $LCA$ and $LCB_c$ for seams of different orientations for 5 m seam	224
Fig. 7.14	Impact of seam location on $I_f$ , for $LCA$ and $LCB_c$ for seams of different orientations for 10 m seam	224
Fig. 7.15	Impact of seam location on $I_f$ , for $LCA$ and $LCB_c$ for seams of different orientations for 15 m seam	225
Fig. 7.16	Impact of seam location on $I_f$ , for $LCA$ and $LCB_c$ for seams of different orientations for 20 m seam	225
Fig. 7.17	Impact of $\theta_s$ on $I_f$ , for $LCA$ and $LCB_c$ for seams at different locations along the base of the dam for 20 m seam	226
Fig. 7.18	Major principal stress contours and stress trajectories for a 10 m wide vertical seam at different locations at base of dam, for $LCA$	229
Fig. 7.19	$y$ -displacements for 10 m wide vertical seam at different locations at base of dam, for $LCA$	230

Fig. 7.20	Major principal stress contours and stress trajectories for 10 m wide seam oriented at $120^\circ$ at different locations at base of dam, for $LCB_c$	231
Fig. 7.21	$y$ -displacements for 10 m wide seam at different locations at base of dam, for $LCB_c$	232
Fig. 7.22	Displacement response for different values of $c_s$ for a 20 m wide seam having $\phi_s$ of $15^\circ$ , for $LCA$	234
Fig. 7.23	$I_f$ for different values of $c_s$ for a 20 m wide seam having $\phi_s$ of $15^\circ$ , for $LCA$	234
Fig. 7.24	$I_f$ for different values of $c_s$ for a 20 m wide seam located at $Hl$ and $T$ , for different $\phi_s$ , for $LCA$	238
Fig. 7.25	Displacement response for different values of $c_s$ for a 20 m wide seam for $\phi_s$ of $15^\circ$ , for $LCB_c$	239
Fig. 7.26	$I_f$ for different values of $c_s$ for a 20 m wide seam for $\phi_s$ of $15^\circ$ , for $LCB_c$	239
Fig. 7.27	$I_f$ for different values of $c_s$ for a 20 m wide seam located at $Hl$ and $T$ , for $\phi_s$ , for $LCB_c$	243
Fig. 7.28	Displacement response for different values of $\phi_s$ for a 20 m wide seam having a $c_s$ of 0 MPa, for $LCA$	244
Fig. 7.29	$I_f$ for different values of $\phi_s$ for a 20 m wide seam having a $c_s$ of 0 MPa, for $LCA$	244
Fig. 7.30	$I_f$ for different values of angles of internal friction of seam ( $\phi_s$ ) for a 20 m wide seam located at $Hl$ and $T$ , for different $c_s$ , for $LCA$	247
Fig. 7.31	Effect of $\phi_s$ for seam on $\delta_{ys}$ for 20 m wide seam at various locations at base of dam for $c_s$ of 0 MPa and for $LCB_c$	249
Fig. 7.32	Effect of $\phi_s$ for seam on $I_f$ for 20 m wide seam at various locations at base of dam for $c_s$ of 0 MPa and for $LCB_c$	249
Fig. 7.33	Effect of $\phi_s$ on $I_f$ for a 20 m wide seam at $Hl$ and $T$ of dam for various $c_s$ for $LCB_c$	250
Fig. 8.1	Problem Geometry - 100 m dam on jointed rock foundation, seam orientations and joint set spacing considered in the analysis.	263
Fig. 8.2	Schematic diagram showing the displacements of the dam without seam, with seam and after the installation of plug	268
Fig. 8.3	Major principal stress and stress trajectories for 10 m wide seam of different orientations at the heel of the dam with $\theta_j = 0^\circ$ , for $LCA$	271
Fig. 8.4	Major principal stress and stress trajectories for 10 m wide seam of different orientations at the heel of the dam with $\theta_j = 90^\circ$ , for $LCA$	272
Fig. 8.5	Major principal stress and stress trajectories for 10 m wide seam of different orientations at the heel of the dam with $\theta_j = 0^\circ$ , for $LCB_c$	273

Fig. 8.6	Major principal stress and stress trajectories for 10 m wide seam of different orientations at the heel of the dam with $\theta_j=90^\circ$ , for $LCB_c$	274
Fig. 8.7	$y$ -displacement contours for 10 m wide seam of different orientations at the heel of the dam with $\theta_j=0^\circ$ , for $LCA$	275
Fig. 8.8	$y$ -displacement contours for 10 m wide seam of different orientations at the heel of the dam with $\theta_j=90^\circ$ , for $LCA$	276
Fig. 8.9	$y$ -displacement contours for 10 m wide seam of different orientations at the heel of the dam with $\theta_j=0^\circ$ , for $LCB_c$	277
Fig. 8.10	$y$ -displacement contours for 10 m wide seam of different orientations at the heel of the dam with $\theta_j=90^\circ$ , for $LCB_c$	278
Fig. 8.11	$I_f$ for a 10 m seam at different locations below the base of the dam for a 100 m high dam for $LCA$	281
Fig. 8.12	$I_f$ for a 10 m seam at different locations below the base of the dam for a 100 m high dam for $LCB_c$	283
Fig. 8.13	Average $I_f$ for seam at different widths below base of dam	284
Fig. 8.14	$I_f$ for a seam of different widths and joint set orientation at heel of the dam for a 100 m high dam	287
Fig. 8.15	$I_f$ for a seam of different widths and joint set orientation at toe of the dam for a 100 m high dam	289
Fig. 8.16	Average $I_f$ for seam of different $\theta_s$ below base of dam	290
Fig. 8.17	Average $I_f$ for seam at different locations below base of dam	293
Fig. 8.18	Average $I_f$ for seam of different joint set orientation below base of dam	295
Fig. 8.19	$I_f$ for 10 m wide seam of different orientations below base of dam with variation of foundation-joint set orientation	297
Fig. 8.20	Major principal stress and stress trajectories for 10 m wide vertical seam at the heel of the dam with $\theta_j=0^\circ$ with different plug depths, for $LCA$	299
Fig. 8.21	$y$ -displacement contours for 10 m wide vertical seam at the heel of the dam with $\theta_j=0^\circ$ with different plug depths, for $LCA$	300
Fig. 8.22	Plug efficiency curve for a vertical seam of 10 m width located at heel of the dam base, for $LCA$ , dam height 100 m and $\theta_j=45^\circ$	302
Fig. 8.23	Plug efficiency at various plug depths for different $\theta_j$ for 10 m $90^\circ$ seam at heel of a 100 m high dam for $LCA$	304
Fig. 8.24	Plug efficiency at various plug depths for different $\theta_j$ for 10 m $90^\circ$ seam at heel of a 100 m high dam for $LCB_c$	304
Fig. 8.25	Optimum plug depth at various seam widths for different seam locations for a 100 m high concrete gravity dam	309

Fig. 8.26	Plug efficiency at various plug depths for 5 m seam of orientation 90° at heel of a 50 m high dam for <i>LCA</i>	309
Fig. 8.27	Plug efficiency at various plug depths for 12.5 m seam of orientation 90° at heel of a 125 m high dam for <i>LCA</i>	310
Fig. 8.28	Plug efficiency at various plug depths for 17.5 m seam of orientation 90° at heel of a 175 m high dam for <i>LCA</i>	310
Fig. 8.29	Plug efficiency at various plug depths for 20 m ( $H/10$ ) seam of orientation 90° at heel of a 200 m high dam for <i>LCA</i>	211
Fig. 8.30	Plug efficiency at various plug depths for 15 m ( $H/5$ ) seam of orientation 90° at heel of a 75 m high dam for <i>LCA</i>	311
Fig. 8.31	Plug efficiency at various plug depths for 10 m ( $H/15$ ) seam of orientation 90° at heel of a 150 m high dam for <i>LCA</i>	312
Fig. 8.32	Plug efficiency at various plug depths for 10 m seam ( $H/20$ ) of orientation 90° at heel of a 50 m high dam for <i>LCA</i>	312
Fig. 8.33	Plots of plug depth ( $D$ ) with respect to seam width ( $B$ ) for dams of various heights	314
Fig. 8.34	Plots of plug depth ( $D$ ) with respect to potential independent variables	317
Fig. 8.35	Plot of comparison between observed plug depth values and estimated plug depth values	318
Fig. 8.36	Plot of residuals for the regression analysis	318
Fig. 8.37	Comparison of results of present study with USBR formula and relation by Gupta (2013)	319
Fig. 8.38	Comparison of observed and predicted optimum plug depth for validation cases	322

## LIST OF TABLES

Table 2.1	Partial Factors of Safety on Shear Strength Parameters (IS 6512, 1984)	11
Table 2.2	Permissible tensile stresses under various load combinations (IS 6512, 1984)	14
Table 2.3	Typical values of Young's modulus of rock mass (in GPa) for nine common rock types (Johnson and Degraff, 1988)	15
Table 2.4	Typical values of Poisson's ratios for nine common rock types (Johnson and Degraff, 1988)	15
Table 2.5	List of dams with stabilization techniques used for foundation remedial measures (Wyllie, 1999)	31
Table 2.6	Critical review of some of the Indian dams	33
Table 2.7	Critical review of some of the dams from outside India	36
Table 2.8	Analytical and numerical studies on dam-foundation system	37
Table 3.1	Block constitutive models in UDEC (Itasca 2011)	56
Table 3.2	Joint constitutive models in UDEC (Itasca, 2011)	58
Table 3.3	Material Properties:	67
Table 3.4	Interface Properties:	68
Table 3.5	Comparison of Results for major and minor principal stresses for <i>LCA</i> - UDEC and $RS^2$	71
Table 3.6	Comparison of results for major and minor principal stresses for <i>LCB</i> - UDEC and $RS^2$	72
Table 3.7	Displacements of dam crest using UDEC and $RS^2$ for Intact Rock foundation:	75
Table 4.1	Apparent dip of major joint sets for Hydro Electric Projects in Himalayas	78
Table 4.2	Material parameters adopted in the present study (Gupta, 2013)	85
Table 5.1	Material parameters adopted for the present study	103
Table 5.2	Angle of resultant, $\theta_r$ , for $LCB_c$	106
Table 5.3	Uplift forces for $LCB_c$	108
Table 5.4	Factor of safety against sliding for $LCB_c$	109
Table 5.5	Percentage variation of principal stresses at the toe for $LCB_c$ and $LCB_u$	123
Table 5.6	Stress-deformation response for Case I (a)	162
Table 5.7	Stress-deformation response for Case I (b)	163
Table 5.8	Stress-deformation response for Case I (c)	164
Table 6.1	Angle of resultant of forces for $LCB_c$	167
Table 6.2	Uplift forces for $LCB_c$ and $LCB_u$	171
Table 6.3	Factor of safety against sliding for $LCB_c$ and $LCB_u$	171

Table 6.4	Critical cases for each of the joint set orientation as the orientation of the other set of joints is changed	198
Table 6.5	Percentage variation of major principal stresses at the toe for $LCB_c$ and $LCB_u$	201
Table 6.6	Incremental $y$ -displacements at heel and toe of dam (over $LCA$ ) for $LCB_c$ and $LCB_u$ and percentage variation in $y$ -displacements for 0.5 m joint set spacing.	202
Table 6.7	Stress-deformation response for dam-foundation with two sets of joints.	203
Table 7.1	Material parameters adopted for shear seam in equivalent continuum rock foundation	208
Table 7.2	Seam influence factor, $I_f$ , for $LCA$ , for $c_s$ of 0.5 MPa and $\phi_s$ of $30^\circ$	211
Table 7.3	Seam influence factor, $I_f$ , for $LCB_c$ , for $c_s$ of 0.5 MPa and $\phi_s$ of $30^\circ$	212
Table 7.4	Average seam influence factor, $I_f$ , for all seam widths for $LCA$	213
Table 7.5	Average seam influence factor, $I_f$ , for all seam widths for $LCB_c$	213
Table 7.6	Percentage change in $I_f$ due to variation in seam width for $LCA$	213
Table 7.7	Percentage change in $I_f$ due to variation in seam width for $LCB_c$	214
Table 7.8	Observations for $LCA$	222
Table 7.9	Observations for $LCB_c$	223
Table 7.10	Overall observations for both loading conditions	223
Table 7.11	Percentage change in $\delta_{ys}$ and $I_f$ due to variation in $c_s$ for $LCA$	235
Table 7.12	Percentage change in $\delta_{ys}$ and $I_f$ due to variation in $c_s$ for $LCB_c$	241
Table 7.13	Percentage change in $\delta_{ys}$ and $I_f$ due to variation $\phi_s$ for $LCA$	245
Table 7.14	Percentage change in $\delta_{ys}$ and $I_f$ due to variation in $\phi_s$ for $LCB_c$	251
Table 7.15	Percentage change in $I_f$ due to variation in seam width for $LCA$	253
Table 7.16	Average seam influence factor for $LCA$ , averaged for different $c_s$ and $\phi_s$	254
Table 7.17	Average seam influence factor for $LCB_c$ , averaged for different $c_s$ and $\phi_s$	255
Table 7.18	Summary of impact of seam width, orientation and location on seam influence factor ( $I_f$ )	258
Table 7.19	Summary of impact of angle of internal friction of seam ( $\phi_s$ ) and seam cohesion ( $c_s$ ) on seam influence factor ( $I_f$ )	259
Table 8.1	Material parameters adopted for shear seam in jointed rock foundation with single set of joints	264
Table 8.2	Percentage variation in highest and lowest $I_f$ across all seam widths for a particular combination of loading condition and seam location	284
Table 8.3	Percentage variation in highest and lowest $I_f$ across all seam widths for a particular combination of loading condition and $\theta_s$	285

Table 8.4	Percentage variation in highest and lowest $I_f$ across all seam widths for a particular combination of loading condition and joint set orientation	285
Table 8.5	Percentage variation in highest and lowest $I_f$ across all $\theta_s$ for a particular combination of loading condition and seam location	291
Table 8.6	Percentage variation in highest and lowest $I_f$ across all $\theta_s$ for a particular combination of loading condition and seam width	291
Table 8.7	Percentage variation in highest and lowest $I_f$ across all $\theta_s$ for a particular combination of loading condition and joint set orientation	292
Table 8.8	Percentage variation in highest and lowest $I_f$ across all seam locations for a particular combination of loading condition and seam width	293
Table 8.9	Percentage variation in highest and lowest $I_f$ across all seam locations for a particular combination of loading condition and $\theta_s$	294
Table 8.10	Percentage variation in highest and lowest $I_f$ across all seam locations for a particular combination of loading condition and joint set orientation	295
Table 8.11	Percentage variation in highest and lowest $I_f$ across all joint set orientations for a particular combination of loading condition and seam location	296
Table 8.12	Percentage variation in highest and lowest $I_f$ across all joint set orientations for a particular combination of loading condition and seam width	298
Table 8.13	Percentage variation in highest and lowest $I_f$ across all joint set orientations for a particular combination of loading condition and $\theta_s$	298
Table 8.14	$y$ -displacements at mid-point of seam and corresponding plug efficiencies observed for different plug depths for a 10 m vertical seam at heel for LCA	301
Table 8.15	Average optimum plug depth estimated for vertical 10 m seam at heel of the dam	305
Table 8.16	Average optimum plug depth estimated for different seam widths	305
Table 8.17	Average optimum plug depth estimated for different loading condition	306
Table 8.18	Average optimum plug depth estimated for different $\theta_s$	306
Table 8.19	Average optimum plug depth estimated for different seam locations	307
Table 8.20	Average optimum plug depth estimated for different joint set orientations	308
Table 8.21	Optimum plug depth estimated for different seam dam height and seam widths	313
Table 8.22	Comparison of optimum plug depth estimated for different seam dam height and seam widths with USBR equation and relation by Gupta (2013)	320
Table 8.23	Comparison of observed and calculated optimum plug depth for validation cases	323
Table 8.24	Impact of variation in joint set spacing in optimum plug depth	324

Table 8.25	Impact of variation in $\frac{E_r}{E_c}$ in optimum plug depth	324
Table 8.26	Impact of variation in $\frac{E_r}{E_s}$ in optimum plug depth	325
Table 8.27	Summary of impact of seam width, orientation, location and joint set orientation on seam influence factor ( $I_f$ )	327

## LIST OF SYMBOLS AND ACRONYMS

$\delta_y$	Vertical displacement without seam
$\delta_{yp}$	Vertical displacement at mid-point of seam with concrete plug
$\delta_{ys}$	Vertical displacement at mid-point of seam without concrete plug
$\phi$	Friction angle
$\phi_b$	Basic friction angle
$\phi_j$	Joint friction angle
$\phi_r$	Effective friction angle
$\phi_s$	Angle of internal friction for shear seam material
$\phi_c$	Concrete friction angle
$\mu$	Dynamic viscosity of the fluid
$\eta_p$	Efficiency of the concrete plug
$\nu$	Poisson's ratio
$\nu_m$	Rock mass Poisson's ratio
$\nu_r$	Intact rock Poisson's ratio
$\rho$	Density
$\sigma_1$	Major principal stress
$\sigma_1^H$	Major principal stress at heel of the dam
$\sigma_1^T$	Major principal stress at toe of the dam
$\sigma_2$	Intermediate principal stress
$\sigma_3$	Minor principal stress
$\sigma_3^H$	Minor principal stress at heel of the dam
$\sigma_3^T$	Minor principal stress at toe of the dam
$\sigma_{Heel}$	Stress at the heel of the dam
$\sigma_n$	Normal stress
$\sigma_r$	Radial stress
$\sigma_T$	Stress at point of discontinuity for bilinear model
$\sigma^t$	Tensile strength
$\sigma_{max}^t$	Maximum allowable tensile strength
$\sigma_{Toe}$	Stress at the toe of the dam

$\sigma_{zz}$	Out-of-plane stress
$\tau_s$	Shear stress
$\theta_k$	Joint set orientation joint set with horizontal
$\theta_j$	Joint set orientation
$\theta_r$	Angle of resultant forces (from upstream horizontal)
$\theta_s$	Seam orientation
$\psi$	Dilation angle
$\psi_j$	Dilation angle of joint
$\Delta p$	Change in pressure across the joint
$\Delta\sigma_n$	Normal stress increment
$\Delta u_n$	Normal displacement increment
$\Delta u_s$	Total incremental shear displacement
$\Delta u_s^e$	Elastic component of shear displacement
$a_0$	Joint aperture at zero normal stress
$a$	Contact hydraulic aperture
$a_{min}$	Residual joint aperture
$A$	Contact area under consideration
$B$	Width of the weak rock seam
$B_d$	Base width of dam
$c$	Cohesion
$c_c$	Concrete cohesion
$c_j$	Joint cohesion
$c_s$	Seam cohesion
$D$	Depth of plug
$e$	Eccentricity with centre of section
$E$	Elastic modulus
$E_c$	Concrete elastic modulus
$E_r$	Young's modulus for intact rock
$E_m$	Young's modulus for rock mass
$\frac{E_r}{E_c}$	Ratio of Young's modulus of intact rock blocks to that of dam concrete

$\frac{E_r}{E_s}$	Ratio of Young's modulus of rock blocks to that of shear seam blocks
$F$	Constant force for body at instant of time
$F_s$	Factor of safety against sliding
$F_H$	Total horizontal force acting on the dam
$F_\phi$	Partial factor of safety in respect of friction
$F_c$	Partial factor of safety in respect of cohesion
$f_c$	Compressive strength of concrete
$f^s$	Shear yield function
$f^t$	Tensile yield function
$G$	Shear modulus
$G_r$	Shear modulus for intact rock
$G_m$	Shear modulus for rock mass
$g^s$	Shear potential function
$H$	Height of the dam above foundation level
$i$	Angle of asperities
$I_f$	Influence factor
$J_f$	Joint factor
$K$	Bulk modulus
$k_0$	In-situ stress ratio
$k_j$	Joint permeability factor
$k_n$	Joint normal stiffness
$k_s$	Joint shear stiffness
$k_{nk}$	Joint normal stiffness of $k^{\text{th}}$ joint set
$k_{sk}$	Joint shear stiffness of $k^{\text{th}}$ joint set
$k_{ni}$	Interface normal stiffness
$k_{si}$	Interface shear stiffness
$l$	Length assigned to the contact between the domains
$m$	Mass
$n$	Number of joints
$q$	Flow rate through joints

$r$	Distance from the point of load application
$R^2$	Correlation coefficient
$s$	Spacing of discontinuity / Joint set spacing
$\bar{s}$	Distance
$s_k$	Joint set spacing joint set
$t$	Time
$U$	Total uplift force
$\dot{u}$	Velocity
$u_n$	Joint normal displacement
$u_s$	Shear displacement
$u_{cs}$	Critical shear displacement
$\sum V$	Sum of all vertical forces
$v_0$	Initial velocity
$v$	Final velocity
$W$	Total weight of dam
$X$	load perpendicular to the surface but parallel to the plane of discontinuity
$Y$	Load parallel to the surface but parallel to the plane of discontinuity
$LCA$	Construction condition (loading condition 'A')
$LCB$	Full reservoir condition (loading condition 'B')
$LCB_c$	Coupled hydro-mechanical loading condition 'B'
$LCB_u$	Uncoupled hydro-mechanical loading condition 'B'
$L_n$	In-situ block size
$L_o$	Block size of 100 mm lab specimen
$C$	Position of seam centre of the dam
$CT$	Position of seam center-toe of the dam
$Hl$	Position of seam at heel of the dam
$HC$	Position of seam heel-centre of the dam
$JCS$	Joint compressive strength
$JCS_o$	Joint compressive strength for 100 mm lab specimen
$JCS_n$	Joint compressive strength for $L_n$ size lab specimen

<i>JRC</i>	Joint roughness coefficient
<i>JRC<sub>o</sub></i>	Joint roughness coefficient for L <sub>0</sub> size lab specimen
<i>JRC<sub>n</sub></i>	Joint roughness coefficient for L <sub>n</sub> size lab specimen
<i>T</i>	Position of seam toe of the dam
<i>GSI</i>	Geological strength index
<i>RMR</i>	Rock mass rating
<i>RQD</i>	Rock quality designation